Five-Hundred Meter Aperture Spherical Radio Telescope (FAST) Cable-Suspended Robot Model and Comparison with the Arecibo Observatory

Arecibo, Puerto Rico Observatorio

Proposed FAST Observatory in China

Robert L. Williams II, Ph.D.
williar4@ohio.edu
Mechanical Engineering
Ohio University

November 2015

For referencing this document, please use:

R.L. Williams II, "Five-Hundred Meter Aperture Spherical Radio Telescope (FAST) Cable-Suspended Robot Model and Comparison with the Arecibo Observatory", Internet Publication, www.ohio.edu/people/williar4/html/pdf/FAST.pdf, July 2015.

FIVE-HUNDRED METER APERTURE SPHERICAL RADIO TELESCOPE CABLE-SUSPENDED ROBOT MODEL AND COMPARISON WITH THE ARECIBO OBSERVATORY

Robert L. Williams II, Ph.D.
Mechanical Engineering, Ohio University, Athens, Ohio, USA
williar4@ohio.edu

ABSTRACT

This paper first presents a comprehensive comparison of the established radio telescope near Arecibo, Puerto Rico vs. the designed Chinese **F**ive-hundred meter **A**perture **S**pherical **T**elescope (FAST) that includes a six-degrees-of-freedom (dof) underconstrained cable-suspended robot to position and orient its focus cabin. Then a straight-line cable model is presented for the FAST robot kinematics and statics, intended as a baseline for the more complicated model including cable sag. However, in the course of examples it was discovered that the straight-line model is of no use since it always yields some negative cable tensions over the required FAST workspace. Therefore, two alternative cable-arrangement designs are presented for FAST which overcome the problem of negative cable tensions when using the straight-line cable pseudostatics model.

KEYWORDS

Five-hundred meter aperture spherical radio telescope, FAST, cable-suspended robot, tendon-driven robot, wire-driven manipulator, inverse pose kinematics, statics model, pseudostatics solution, Arecibo Observatory.

1. INTRODUCTION

Earth-based radio telescopes are used for observations of the earth's atmosphere, the solar system, and deep space objects and systems. The Arecibo Observatory in Puerto Rico is the largest radio telescope in the world, in continuous operation since its completion in 1963. The Arecibo radio telescope is scheduled to be surpassed by a much larger earthbound radio telescope, the **F**ive-hundred meter **A**perture **S**pherical **T**elescope (FAST) currently under development in China, with a 2016 target completion date. The Square Kilometer Array (SKA) concept is an international effort. It will consist of thousands of smaller antennae over 3,000 km, with a total collection area of 1 km^2, and it will exist in South Africa and Australia (skatelescope.org). Though their SKA proposal was not accepted, the Chinese decided to go ahead with construction of FAST as a single-site SKA facility.

The Arecibo Radio Telescope is huge (305 m diameter spherical cap reflector) – and FAST is significantly larger (five-hundred meter is a slight misnomer, since it has a 520 m diameter spherical cap reflector). While the Arecibo design is based on a cable-suspended ***structure*** with two-degrees-of-freedom (dof) for receiver pointing, the larger size of FAST is enabled by the use of a six-cable-suspended ***robot*** design for six-dof positioning and orienting of the focus cabin relative to the reflector surface.

One of the better known cable robots is the Skycam, which dynamically positions a video camera for use in sports stadiums (Cone, 1985). The cable robot RoboCrane and many related systems were developed at NIST (Albus et al., 1993). Cable-suspended robots have been proposed for International Space Station (Campbell et al., 1995) and large outdoor construction (Bosscher et al., 2007). A group unrelated to the FAST project (Meunier et al., 2009) presents pose control for a large Canadian radio telescope concept; the cable-suspended robot is overconstrained (with actuation redundancy so the role of gravity is less important) and the focus cabin is suspended by an aerostat.

Cable robots are relatively simple in form, with multiple cables attached to a mobile platform or end-effector. The end-effector is manipulated by motors that can extend or retract the cables. In addition to large workspaces, cable robots are relatively inexpensive, fast, lightweight, and stiff. Two major control issues exist that do not apply to conventional rigid-link robots: the cables can only apply tension (unidirectional tension actuation) and large-scale cable robots are subject to cable sag.

The six-cable-suspended FAST robot is classified as underconstrained, meaning that the six cables alone are not sufficient, but gravity is also required to achieve pseudostatic equilibrium at the various poses.

The FAST Project has been under development since 1994, by the National Astronomical Observatories of Beijing, China. The simulation and design of the six-cable-suspended robot subsystem has been in collaboration with Universitat Darmstadt, Germany. FAST has been published often (e.g. Nan et al., 2011; Nan 2006), including cable sag and elasticity (Li et

al., 2013; Kozak et al., 2006), workspace and stable poses (Li et al., 2008), and *XYZ* trajectory control (no orientation control, Strah et al., 2008).

The motivation for the current paper is two-fold: 1. To present a comparison of the FAST to the Arecibo Radio Telescopes, which has not been previously published; and 2. To present a complete model for the FAST six-cable-suspended robot in one publication. The various papers by the principals on the FAST Project are incomplete and sometimes contradictory (presumably due to design changes over time).

The current paper first presents a comparison of the existing Arecibo and proposed FAST Radio Telescope facilities. Then the FAST cable-suspended model is described and summarized. This is followed by the Inverse Pose Kinematics Solution, a discussion of the Forward Pose Kinematics Solution, and then the Inverse Pseudostatics Solution. The paper then presents examples for the presented models, including a trajectory example. The assumptions of straight cables (no sag) and no loss in positive cable tensions are made, to provide a baseline model with which to compare the more complicated cable sag/elasticity models of the FAST Project.

2. ARECIBO AND FAST COMPARISON

This section presents an overall comparison of the existing radio telescope near Arecibo, Puerto Rico and the proposed FAST radio telescope in China. The Arecibo information came from a personal visit of the author to the site in September 2014, from the excellent Angel Ramos Foundation Visitor Center. Most of this information is also available in various websites via Google searches. The FAST information came from Nan et al. (2011), Nan (2006), Li et al. (2013), Kozak et al. (2006), Li et al. (2008), and Strah et al. (2008), plus from various websites via Google searches.

2.1 Arecibo Radio Telescope

The Observatorio de Arecibo (the William E. Gordon Telescope, Figure 1) is located 12 miles south of Arecibo, Puerto Rico in a karst sinkhole (on a former tobacco farm), at latitude 18° 20' N and longitude 66° 45' W, and 497 m above sea level. It was built between 1960-1963 for $9.3M ($71.3M in 2014 USD), funded by the U.S. government. Called the National Astronomy and Ionosphere Center, it has had three functions (which continue):

- Study earth's atmosphere up to space
- Study planets and asteroids
- Study deep space stars

Figure 1. General View of the Arecibo Observatory
wikipedia.org

The reflector is a partial sphere of 253.6 m diameter composed of 39,000 individually-shaped panels. The reflector is stationary (though it may be shaped to maintain sphericity) and the overhead receiver moves to point the radio waves sensor. Workers, limited to 135 lb, wear special snowshoe-like shoes to walk the reflector for maintenance and repairs. The planar partial spherical cap has a 304.8 m (length of 2.9 futbol pitches) diameter at "ground" level (the karst sinkhole long ago removed that ground). The partial spherical cap reflector has a 73,000 m^2 collecting area and depth of 50.9 m. There are 3 reinforced concrete towers of 110, 80, and 80 m high (so their heights above sea level are equal), on the vertices of an equilateral triangle with side 379.8 m. The towers support a static 1,000 ton (U.S. tons – 907,185 kg) equilateral-triangular platform of side 66.7 m, 45.7 m above "ground" level. The static equilateral-triangular platform is aligned (oriented) identically with the equilateral-triangular base of towers. The planar partial spherical cap and the equilateral triangles of the base towers and the suspended platform share a common center (from the top view).

A total of 39 steel twisted cables support the suspended platform statically, with a total cable length of 6.4 km. Each one of the 39 cables has a mass of 9,072 kg and a diameter of 8.3 cm. The associated cable unit weight is about 481.6 N/m. To the author's eye, all cables were perfectly tensioned, i.e. no cable sag was evident. The Arecibo platform is static, i.e. not controlled by a cable-suspended robot. However, due to wear and temperature changes, there is an active control system with three pairs of vertical cables to each vertex of the suspended platform to ensure platform horizontality to within a millimeter. The three independent motors for this are ground-mounted and the control cables run through the partial spherical reflector.

The platform has a two-dof subsystem mounted under it. The 93 m long bow-shaped track called the azimuth arm (see Figure 2), rotates fully about the vertical axis. Then the receiver dome can rotate $\pm 20^\circ$ from nominal in a perpendicular plane, oriented first by the azimuth arm rotation. The fixed partial-spherical curvature mirror focuses radio waves into a line above reflecting dish, and this line is further focused to a single point by additional mirrors.

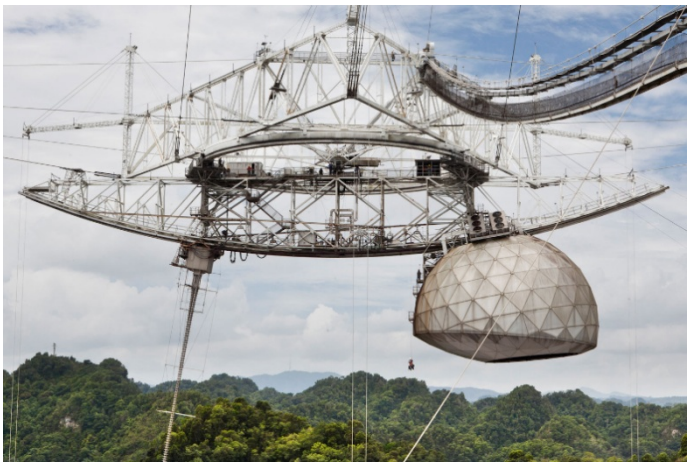

Figure 2. Arecibo Observatory 2-dof Azimuth Arm
www.gravitec.com

Among the Arecibo Observatory's many accomplishments, the first pulsar in a binary system was discovered in 1974, providing a confirmation of Einstein's theory of general relativity and leading to a 1993 Nobel Prize for astronomers Taylor and Hulse. The 'Arecibo Message' was sent into outer space in 1974. The Arecibo Radio Telescope has been featured in popular media, including the Hollywood films Contact (1997) and James Bond's Goldeneye (1995).

2.2 FAST Radio Telescope

The proposed **F**ive-hundred meter **A**perture **S**pherical **T**elescope (FAST, see Figure 3) is currently under development in the Dawodang karst depression in south Guizhou Province in southern China, at latitude $25^\circ\ 48'$ N and longitude $107^\circ\ 21'$ E, at 1,000 m above sea level. Like the Arecibo Observatory location, this site is remote and radio-quiet. The karst sinkhole was 98% shaped to the designed spherical cap reflector already, requiring little dirt/rock removal. The estimated completion cost is $108M (2014 USD), funded by the Chinese government.

Figure 3. FAST CAD Model Overlaid on Site
Nan et al. (2011)

FAST is designed to improve sharpness of images relative to Arecibo in four areas:

- Interstellar gas
- Pulsars
- Supernovae
- Black hole emissions

FAST is supposed to enable the following new investigations:

- Neutral hydrogen in Milky Way and other galaxies
- Detection of new galactic and extragalactic pulsars
- Search for the first shining stars
- Search for extraterrestrial life (Arecibo has been used for this also).

As seen in Figure 4, the FAST reflector is a partial sphere of $R_F = 300$ m radius composed of 4,400 panels (of only 187 individual types). The reflector is stationary but real-time active control of a cable-net structure is used to form a parabolic mirror anywhere within the spherical cap. Also in Figure 4, the virtual focus surface partial sphere radius is $R_V = 160$ m. The FAST system parabolic mirror is the size of the entire Arecibo reflector, 305 m (Arecibo can only use 221 m of its 305 m dish at one time). Like Arecibo, the FAST overhead receiver (focus cabin) moves to position and orient the radio waves sensor, but unlike Arecibo, this is controlled by a six-dof, six-cable-suspended robot. The planar partial spherical cap of the reflector has a diameter of $d_R = 2R_F \sin(60^\circ) = 519.6$ m (length of 4.9 futbol pitches) at "ground" level. This diameter is 1.7 times the Arecibo diameter. It is significantly (4%) larger than the 500 m claimed in the name 'FAST'. The planar partial spherical cap of the virtual focus surface has a diameter of $d_V = 2R_V \sin(40^\circ) = 205.7$ m. The partial spherical cap reflector has a collecting area of approximately 1 km^2 and a depth of $H = R_F(1 - \cos(60^\circ)) = 150$ m. The six cable-support towers

each have heights of $h = 150$ m, on the vertices of a regular hexagon inscribed in a circle of radius $r_F = 300$ m (not the same dimension as R_F, though they have the same value; see Figure 7a). The six towers/cables must support a 'lightweight' active focus cabin mass of about 30 metric tons (the Arecibo suspended triangular platform is greater than 30 times more massive), from $h - R_V = -10$ (10 m below ground level) to $h - R_V \cos(40^\circ) = 27.4$ m above ground level (see Figure 4). If FAST were designed as Arecibo, 10,000 metric tons of suspended metal would be required.

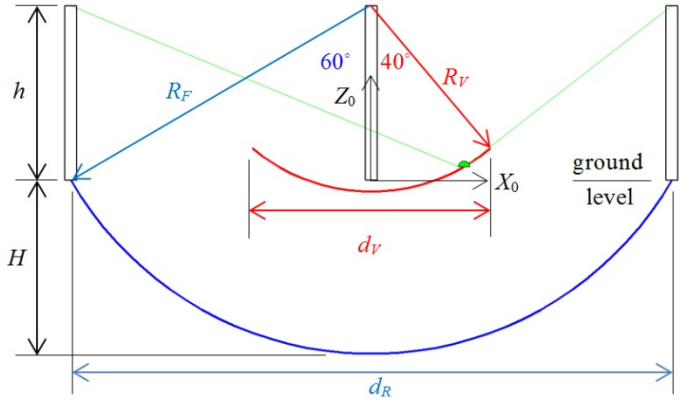

Figure 4. FAST Front View

As shown in Figure 5, each of the six steel cables connecting the FAST focus cabin to the base towers is a complicated design, to allow the 6-dof control and running power and signal cables along the same route. Each of the six cables has a unit weight of 176.4 N/m and a diameter of 4.2 cm. Compared to the Arecibo cables (of which there are 39), the FAST cables are half the diameter and about one-seventh of the unit weight. Even with the larger size of FAST, Arecibo has a significant amount of cable mass in the air compared with FAST. Each of the six FAST cables provides 120 – 280 kN in tension, with a load limit of 1200 kN. The first-mode mechanical resonance of each cable is 0.18 Hz and the cable Young's Modulus is 1.7×10^5 MPa. Each tower incorporates a counterweight to assist in cable tensioning.

The FAST focus cabin, whose pose in space is controlled by the six active cables, is used as the coarse positioning/orienting system. A 6-dof rigid-link Stewart Platform (see Figure 6) actuated by six prismatic joints is mounted to the underside of the focus cabin to accomplish fine positioning/orienting relative to the cable-suspended focus cabin. The macro-manipulator is capable of accuracy on the order of 10 cm, while the micro-manipulator is capable of accuracy on the order of 10 mm. This forms an interesting macro-/micro-manipulator system consisting of two parallel (one cable, one rigid) robots in series. The Stewart Platform is capable of lifting 3 metric tons.

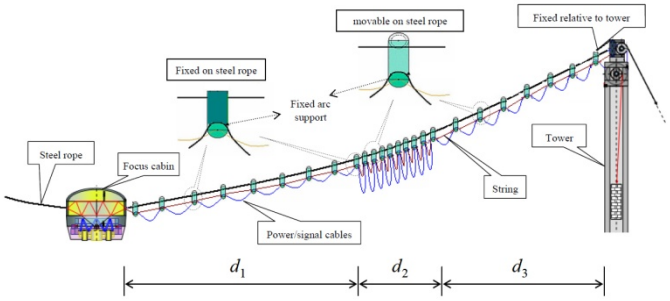

Figure 5. FAST Cable Design
Nan et al. (2011)

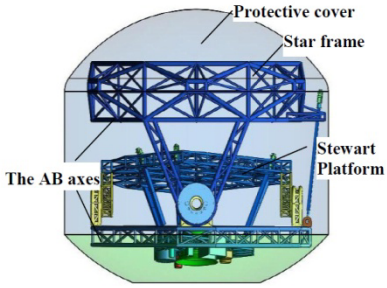

Figure 6. FAST Focus Cabin/Stewart Platform
Nan et al. (2011)

An approximately 1/10th scale 50 m diameter hardware FAST model has been built and is being tested at Miyun Station in China.

2.3 Arecibo vs. FAST Characteristics

To conclude this comparison of the Arecibo and FAST Radio Telescopes, here are some more facts.

- FAST will see 3 times further into space than Arecibo; FAST will have capabilities up to 1,000 light years.
- FAST will survey 10 times faster than Arecibo.
- FAST has a collecting area more than twice as large as Arecibo.
- Arecibo points straight up with a $\pm 20^\circ$ cone of coverage from the zenith; it has a 10 GHz bandwidth.
- FAST is south-pointing with a $\pm 40^\circ$ cone of coverage from the zenith; it has a 3 GHz bandwidth (with possible future upgrade to 5GHz).
- The 39 10-U.S.-ton cables of Arecibo are massive, weighing a total of 3,506.2 kN, yet are maintained with tension (i.e. no cable sag). The 6 active cables of FAST are relatively lightweight, weighing a total of 513.8 kN (15% of the Arecibo cables' weight, a nominal value that changes slightly with FAST motion), yet cable sag is taken into account (see Figure 5). This is based on a FAST unit cable weight of 176.4 N/m (for "normally stretched cables", Li et al., 2013).

The Appendix presents MATLAB graphics to scale for size comparison of the Arecibo and FAST Radio Telescopes.

3. FAST CABLE-SUSPENDED ROBOT DESCRIPTION

This section presents a description of the six-cable-suspended FAST positioning/orienting robot. This six-dof robot is responsible for the *XYZ* translational and the roll-pitch-yaw rotational control of the FAST focus cabin within its spherical cap virtual focus surface workspace. A rigid-link inverted Stewart Platform parallel robot is used for fine positioning and orienting with respect to the six-dof FAST cabin – this Stewart platform is not considered in the current paper.

Figure 7 shows the FAST six-cable-suspended robot kinematic diagram. The fixed base Cartesian reference frame is {0}, whose origin is located in the center of the base circular (or, regular hexagon), at "ground" level. "Ground" is in quotes because {0} is floating since the karst sinkhole removed the ground long ago – so the {0} origin is level with the bases of the six fixed support towers. The six ground-fixed cable connection points B_i, $i = 1,2,\cdots 6$ are on the tops of the six static support poles, each a height h = 150 m above "ground" level. The cable connection points B_i are the vertices of a regular hexagon inscribed by a circle of radius $r_F = 300$ m. In this model point B_1 is located 30° counter-clockwise from X_0; then the five remaining B_i are located symmetrically by ensuing 60° counter-clockwise rotations. Also evident in Figure 7a is the partial spherical cap reflector radius $r_R = d_R/2$.

The FAST focus cabin is represented in Figure 7b (and 7a) as a circle of diameter $d_{CAB} = 12.8$ m (out of scale in Figures 7 for clarity). The moving Cartesian coordinate control frame for the focus cabin is {*P*}, whose origin is located in the center of the cabin, a distance δ below the plane where the six active cables connect. At zero roll-pitch-yaw orientation, visualize six moving cabin cable connection points P_i, $i = 1,2,\cdots 6$ (only P_1, P_3, P_5 are needed in this model as will be explained shortly). These six potential moving connection points are the vertices of a regular hexagon inscribed by a circle of radius $r_{CAB} = 6.4$ m. In this model point P_1 is located 30° counter-clockwise from X_P; then the five remaining P_i are located symmetrically by ensuing 60° counter-clockwise rotations.

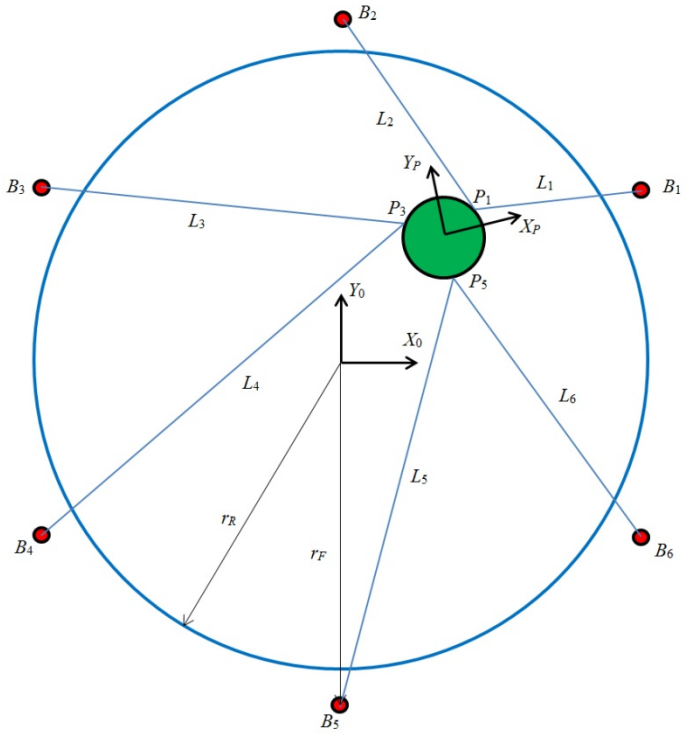

Figure 7a. FAST Top View for all 6 Active Cables

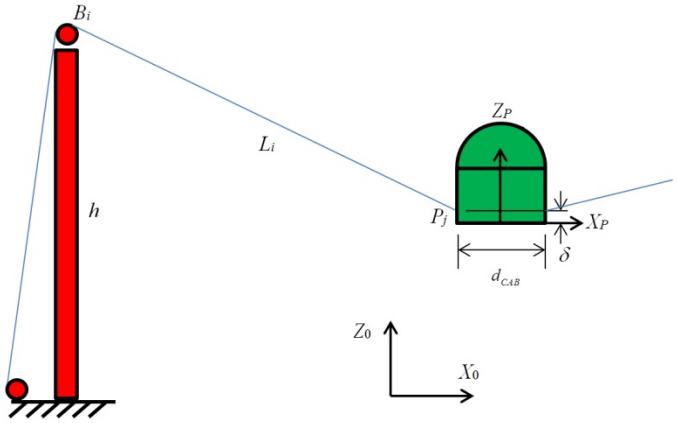

Figure 7b. FAST Front View for Active Cable *i*

Figure 7. Six-Cable-Suspended Robot Diagram

In the FAST CAD model that has been widely published (Figure 3, e.g. Nan et al., 2011), the six cable lengths L_i appear to connect each B_i straight to each P_i, $i = 1,2,\cdots 6$:

B_i	1	2	3	4	5	6
P_j	1	2	3	4	5	6

However, doing so yields a statics Jacobian matrix that is always singular, which is clearly undesirable. Li et al. (2013) show the cable-connection design of Figure 7a, which is adopted in the model of the current paper:

B_i	1	2	3	4	5	6
P_j	1	1	3	3	5	5

As seen in Figure 7a, the six active cable lengths are $\mathbf{L} = \{L_1 \quad L_2 \quad L_3 \quad L_4 \quad L_5 \quad L_6\}^T$, connected as shown in Figure 7a.

As seen in the front view of Figure 7b, each of the six tensioning torque motors/cable reels is fixed to the ground. Each of the six active drive cables runs from their respective ground-mounted cable reels over pulleys on the six support tower tops at fixed cable support points B_i to moving focus cabin points P_j. Again, the size of the focus cabin is greatly enlarged in Figure 7b for clarity. In Figure 7b the orientation of $\{P\}$ appears to be identical to that of $\{0\}$, for clarity. In fact, the moving focus cabin can be controlled for (limited) roll-pitch-yaw orientation angles with respect to the fixed frame $\{0\}$.

The fixed-base cable connection points B_i are constant in the base frame $\{0\}$:

$$ {}^0\mathbf{B}_i = \{R\cos\psi_i \quad R\sin\psi_i \quad h\}^T \qquad i = 1,2,\cdots 6 \quad (1) $$

$$ \psi_1 = 30^\circ \qquad \psi_4 = 210^\circ $$
$$ \psi_2 = 90^\circ \qquad \psi_5 = 270^\circ $$
$$ \psi_3 = 150^\circ \qquad \psi_6 = 330^\circ $$

Similarly, the focus cabin cable connection points P_j are constant in the moving frame $\{P\}$:

$$ {}^P\mathbf{P}_j = \{r_{CAB}\cos\psi_j \quad r_{CAB}\sin\psi_j \quad \delta\}^T \qquad j = 1,3,5 \quad (2) $$

where $\delta = 0.246$ m is the Z offset from the CG (origin of $\{P\}$) to the cable-connection plane $P_1P_3P_5$ of the focus cabin. The table below summarizes the important, previously-presented FAST robot parameters.

4. FAST INVERSE POSE KINEMATICS SOLUTION

The 6-cable FAST robot inverse pose kinematics (IPK) problem is stated: Given the desired moving focus cabin pose $\left[{}^0_P\mathbf{T}\right]$, calculate the six active cable lengths L_i, $i = 1,2,\cdots 6$. The current IPK model assumes straight cables (no sag) that are always in tension, and ignores cable mass and elasticity. This will serve as a baseline model for the models in Li et al. (2013) and Kozak et al. (2006) which include these items.

name	meaning	value
R_F	reflector sphere radius	300 m
R_V	virtual focus sphere radius	160 m
d_R	reflector cap ground diameter	520 m
d_V	virtual cap planar diameter	206 m
H	reflector cap depth	150 m
h	support tower height (6)	150 m
r_F	support tower circle radius	300 m
d_{CAB}	focus cabin diameter	12.8 m
δ	focus cabin offset	0.236 m
mg	focus cabin weight	294.9 kN

The IPK input $\left[{}^0_P\mathbf{T}\right]$ may be specified in terms of the desired vector location $\left\{{}^0\mathbf{P}_P\right\}$ of the origin of moving frame $\{P\}$ with respect to $\{0\}$, plus three angles representing the orientation of moving frame $\{P\}$ with respect to $\{0\}$. Choosing α-β-γ, *Z-Y-X* Euler Angles (Craig 2005), the associated orthonormal rotation matrix is:

$$ \left[{}^0_P\mathbf{R}\right] = \begin{bmatrix} c\alpha c\beta & -s\alpha c\gamma + c\alpha s\beta s\gamma & s\alpha s\gamma + c\alpha s\beta c\gamma \\ s\alpha c\beta & c\alpha c\gamma + s\alpha s\beta s\gamma & -c\alpha s\gamma + s\alpha s\beta c\gamma \\ -s\beta & c\beta s\gamma & c\beta c\gamma \end{bmatrix} \quad (3) $$

Then the 4x4 homogeneous transformation matrix description of pose is (Craig 2005):

$$ \left[{}^0_P\mathbf{T}\right] = \begin{bmatrix} & \left[{}^0_P\mathbf{R}\right] & & \left\{{}^0\mathbf{P}_P\right\} \\ 0 & 0 & 0 & 1 \end{bmatrix} \quad (4) $$

The solution to the FAST IPK problem may be used as the basis for a pose control scheme, executing pre-planned trajectories and other motions on the virtual focus surface partial-spherical-cap workspace. Like most cable-suspended robots and many parallel robots in general, the FAST IPK solution is straight-forward and poses no computational challenge for real-time implementation. Given the desired moving cabin pose $\left[{}^0_P\mathbf{T}\right]$, we find the moving platform cable connection points P_1, P_3, and P_5. Then the inverse pose solution consists simply of calculating the cable lengths using the Euclidean norm of the appropriate vector differences between the various moving and fixed cable connection points. The IPK solution yields a unique closed-form solution.

Given $\left[{}^0_P\mathbf{T}\right]$ we calculate the moving cable connection points P_1, P_3, and P_5 with respect to the fixed base frame $\{0\}$ using:

$$\left\{ {}^{0}\mathbf{P}_j \right\} = \left[{}^{0}_{P}\mathbf{T} \right] \left\{ {}^{P}\mathbf{P}_j \right\} \qquad j = 1,3,5 \qquad (5)$$

where the $\left\{ {}^{P}\mathbf{P}_j \right\}$ vectors were given in (2). Note we must augment each position vector in (5) with a '1' in the fourth row to make the 4x4 matrix multiplication valid. The FAST straight-cable IPK solution is:

$$\begin{aligned} L_1 &= \left\| {}^{0}\mathbf{B}_1 - {}^{0}\mathbf{P}_1 \right\| & L_2 &= \left\| {}^{0}\mathbf{B}_2 - {}^{0}\mathbf{P}_1 \right\| \\ L_3 &= \left\| {}^{0}\mathbf{B}_3 - {}^{0}\mathbf{P}_3 \right\| & L_4 &= \left\| {}^{0}\mathbf{B}_4 - {}^{0}\mathbf{P}_3 \right\| \\ L_5 &= \left\| {}^{0}\mathbf{B}_5 - {}^{0}\mathbf{P}_5 \right\| & L_6 &= \left\| {}^{0}\mathbf{B}_6 - {}^{0}\mathbf{P}_5 \right\| \end{aligned} \qquad (6)$$

Note the direction of the six cable length vectors in (6) were chosen in the direction of positive cable tensions.

5. FAST FORWARD POSE KINEMATICS

The 6-cable FAST robot forward pose kinematics (FPK) problem is stated: Given the six active cable lengths L_i, $i = 1,2,\cdots 6$, calculate the associated focus cabin pose $\left[{}^{0}_{P}\mathbf{T} \right]$. The FPK solution for cable-suspended robots and other parallel robots is generally very difficult. It requires the solution of multiple coupled nonlinear (transcendental) algebraic equations, from the vector loop-closure equations. Multiple valid solutions generally result.

Referring to Figures 7, we see that the FAST robot FPK problem is identical to the FPK solution for an upside-down 6-3 Stewart Platform (assuming straight cables always under positive tension). The FPK solution is based on identifying 3 known triangles, $B_1P_1B_2$, $B_3P_3B_4$, and $B_5P_5B_6$ (refer to Figure 8). Construct a virtual link to P_j, perpendicular to base line B_iB_{i+1} for each of these three triangles. Imagine rotating each triangle (each virtual link) about B_iB_{i+1}. The FPK solution exists where all three P_j rotate until P_1P_3, P_3P_5, and P_5P_1 are each of the correct, known lengths simultaneously. This solution was presented by Williams (1992). The solution boils down to an 8th-order polynomial, meaning that there are potentially 8 multiple solutions. Even pairs of some of these solutions may be imaginary.

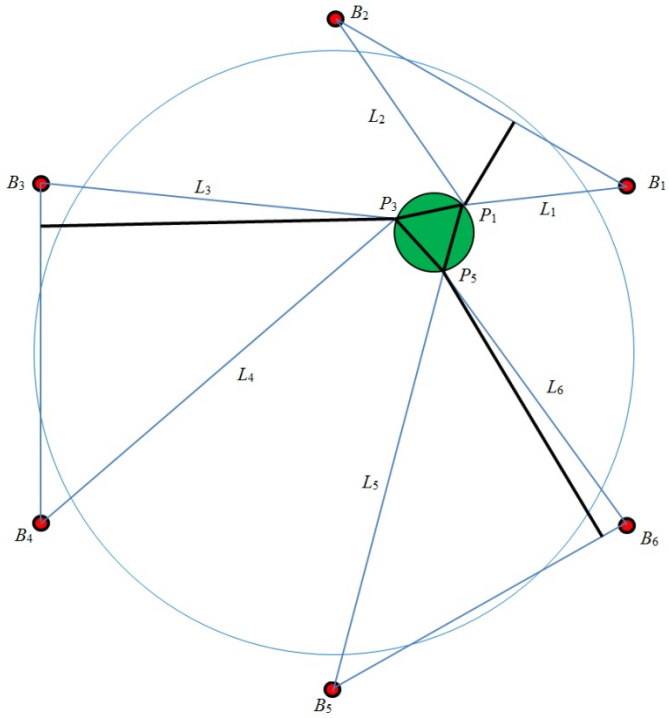

Figure 8. FAST FPK Diagram

6. FAST PSEUDOSTATICS ANALYSIS

To maintain safe and stable control in all motions, all cable tensions must remain positive at all times. Gravity acting on the focus cabin is required to ensure that the six active cables remain in tension, as long as the rotations are not too far from the nominal horizontal orientation. A pseudostatic model is developed in this section and applied to the FAST inverse statics solution.

6.1 Equations for Static Equilibrium

This section presents statics modeling for the six-cable-suspended FAST robot. All six active cables connect in parallel from the fixed base to the moving focus cabin, as shown in Figure 7a. Again we assume straight cables (no sag) that are always in tension, and ignore cable mass and elasticity, so the current model serves as a baseline for Li et al. (2013) and Kozak et al. (2006). In pseudostatics it is assumed that the focus cabin accelerations and velocities are low enough to justify ignoring inertial dynamic effects and use statics equations of equilibrium.

For static equilibrium the vector force sum and vector moment sum of the six active cable tensions plus gravitational loading and external wrench acting on the focus cabin must balance to zero. Figure 9 shows the statics free-body diagram for the focus cabin where *CG* indicates the center of gravity location. The six active cable tension vectors are $\mathbf{t}_i$, $i = 1,2,\cdots 6$.

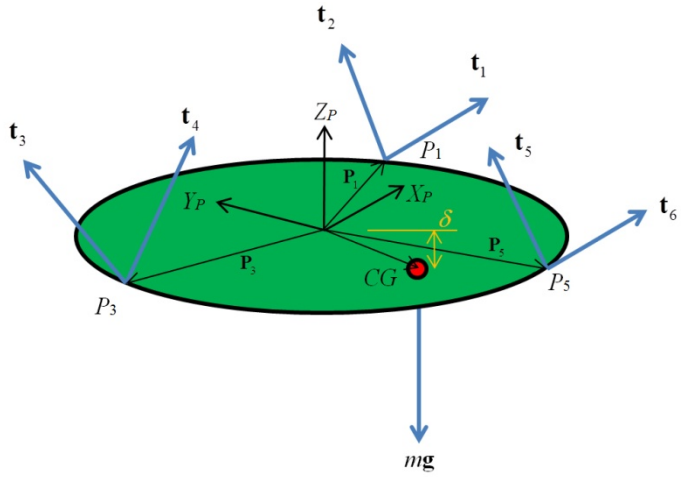

Figure 9. Focus Cabin Statics Free-Body Diagram

The vector force and moment equations of static equilibrium are:

$$\sum_{i=1}^{6}\mathbf{t}_i + m\mathbf{g} + \mathbf{F}_{EXT} = \mathbf{0} \tag{7}$$

$$\sum_{i=1}^{6}\mathbf{m}_i + {}^0_P\mathbf{R}\,{}^P\mathbf{P}_{CG} \times m\mathbf{g} + \mathbf{M}_{EXT} = \mathbf{0} \tag{8}$$

where $\mathbf{t}_i = t_i\hat{\mathbf{L}}_i$ is the vector cable tension applied to the focus cabin by the i^{th} active cable (in the positive cable length direction $\hat{\mathbf{L}}_i$ as established in IPK); m is the total focus cabin mass; $\mathbf{g} = \{0 \quad 0 \quad -g\}^T$ is the gravity vector; $\mathbf{F}_{EXT}$ is the external vector force exerted on the focus cabin by the environment; $\mathbf{m}_i = \left[{}^0_P\mathbf{R}\right]\left\{{}^P\mathbf{P}_j\right\} \times \{\mathbf{t}_i\}$ is the moment due to the i^{th} active cable tension (${}^P\mathbf{P}_j$ is the moment arm from the focus cabin control point P to the i^{th} active cable connection point, expressed in $\{P\}$ coordinates, $j = 1,3,5$); ${}^P\mathbf{P}_{CG}$ is the position vector to the moving platform CG from the moving platform control point P (the origin of $\{P\}$); and $\mathbf{M}_{EXT}$ is the external vector moment exerted on the focus cabin by the environment. Moments are summed about the platform control point P and all vectors must be expressed in a common frame; $\{0\}$ is chosen.

Now we derive the pseudostatics Jacobian matrix based on the vector force and moment statics equations. Substituting the above details into (7) and (8) yields:

$$[\mathbf{S}]\{\mathbf{t}\} = -\{\mathbf{W}_{EXT} + \mathbf{G}\} \tag{9}$$

where $\{\mathbf{t}\} = \{t_1 \quad t_2 \quad \cdots \quad t_6\}^T$ is the vector of active cable tensions, $\{\mathbf{G}\} = \{m\mathbf{g} \quad {}^0_P\mathbf{R}\,{}^P\mathbf{P}_{CG} \times m\mathbf{g}\}^T$ is the gravity wrench vector, $\{\mathbf{W}_{EXT}\} = \{\mathbf{F}_{EXT} \quad \mathbf{M}_{EXT}\}^T$ is the external wrench vector, and the statics Jacobian matrix $[\mathbf{S}]$ is:

$$[\mathbf{S}] = \begin{bmatrix} \hat{\mathbf{L}}_1 & \hat{\mathbf{L}}_2 & \hat{\mathbf{L}}_3 & \hat{\mathbf{L}}_4 & \hat{\mathbf{L}}_5 & \hat{\mathbf{L}}_6 \\ \mathbf{P}_1\times\hat{\mathbf{L}}_1 & \mathbf{P}_1\times\hat{\mathbf{L}}_2 & \mathbf{P}_3\times\hat{\mathbf{L}}_3 & \mathbf{P}_3\times\hat{\mathbf{L}}_4 & \mathbf{P}_5\times\hat{\mathbf{L}}_5 & \mathbf{P}_5\times\hat{\mathbf{L}}_6 \end{bmatrix} \tag{10}$$

where $\mathbf{P}_j = \left\{{}^0\mathbf{P}_j\right\} = \left[{}^0_P\mathbf{R}\right]\left\{{}^P\mathbf{P}_j\right\}$, $j = 1,3,5$.

In nominal performance, the external wrench $\{\mathbf{W}_{EXT}\}$ acting on the focus cabin should be zero; $\{\mathbf{W}_{EXT}\}$ is included in the statics model to include primarily wind loading if desired. Also, the FAST design has the *CG* of the focus cabin located at the origin of the control frame $\{P\}$; but ${}^P\mathbf{P}_{CG}$ is included in the statics model in case that design changes.

6.2 FAST Inverse Pseudostatics Solution

The statics equations (9) can be used in two ways. Given the active cable tensions $\{\mathbf{t}\}$ and the six cable unit vectors $\hat{\mathbf{L}}_i$ from kinematics analysis, forward statics analysis uses (9) directly to verify statics equilibrium. For control, simulation, and valid-tension workspace determination, the more useful problem is inverse statics analysis. This problem is stated: calculate the required active cable tensions $\{\mathbf{t}\}$ given the focus cabin mass and pose, plus all $\hat{\mathbf{L}}_i$. It is solved by inverting (9):

$$\{\mathbf{t}\} = -[\mathbf{S}]^{-1}\{\mathbf{W}_{EXT} + \mathbf{G}\} \tag{11}$$

The statics Jacobian Matrix $[\mathbf{S}]$ is a square 6x6 matrix and hence the standard matrix inverse applies in (11). A unique $\{\mathbf{t}\}$ solution is guaranteed if the robot is not in a singular pose.

Assuming pseudostatic motion, the inertia of the actuator shafts do not enter into the analysis and the statics torque/tension relationship for each of the 6 actuators is $\tau_i = r_i t_i$, $i = 1,2,\cdots 6$, where τ_i is the i^{th} actuator torque, r_i is the i^{th} cable reel radius, and t_i is the i^{th} cable tension.

7. FAST EXAMPLES

Snapshot example 1 for the nominal configuration where the focus cabin is in the center of the workspace, at the nadir of the virtual focus spherical cap surface, with zero orientations:

Given $\left\{{}^0\mathbf{P}_P\right\} = \{0 \quad 0 \quad -10\}^T$ m and $\{\alpha \quad \beta \quad \gamma\} = \{0 \quad 0 \quad 0\}$, the calculated IPK and inverse statics results are:

$$\mathbf{L} = \{334.2 \quad 337.1 \quad 334.2 \quad 337.1 \quad 334.2 \quad 337.1\}^T \text{ m}$$

$$\{\mathbf{t}\} = \{205680 \quad 0 \quad 205680 \quad 0 \quad 205680 \quad 0\}^T \text{ N}$$

Snapshot example 2 for the configuration where the focus cabin is on the edge of the workspace, on top of the virtual focus spherical cap surface, *YZ* plane, with 16° focus cabin tilt angle:

Given $\left\{{}^0\mathbf{P}_P\right\} = \{0 \quad 102.8 \quad 27.4\}^T$ m and $\{\alpha \quad \beta \quad \gamma\} = \{0 \quad 0 \quad 16^\circ\}$, the calculated IPK and inverse statics results are:

$$\mathbf{L} = \{285.2 \quad 229.1 \quad 285.2 \quad 380.6 \quad 415.6 \quad 379.1\}^T \text{ m}$$

$$\{\mathbf{t}\} = \{260550 \quad 17 \quad 363430 \quad -76660 \quad 114920 \quad 59110\}^T \text{ N}$$

Trajectory example where the focus cabin traces the circle of the virtual focus spherical cap surface top (center $\{0 \quad 0 \quad 27.4\}^T$ and radius 102.8 m), with zero orientations $\{\alpha \quad \beta \quad \gamma\} = \{0 \quad 0 \quad 0\}$:

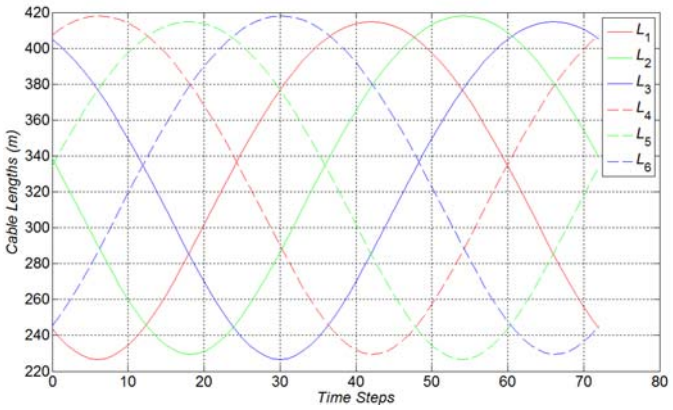

Figure 10a. Trajectory Example Cable Lengths

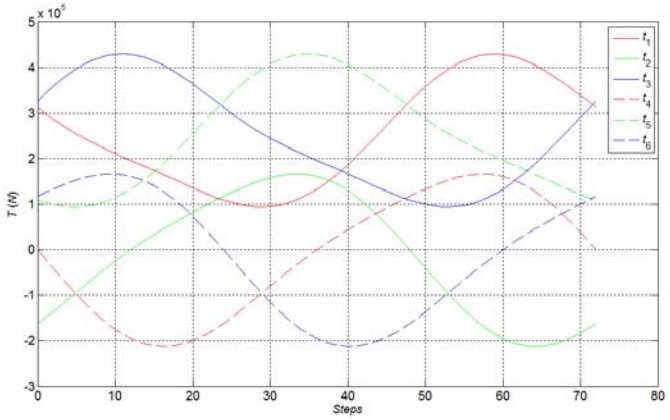

Figure 10b. Trajectory Example Cable Tensions

All examples assume the focus cabin *CG* is located at the control point, the origin of {*P*} so that ${}^P\mathbf{P}_{CG} = \{0 \quad 0 \quad 0\}^T$. Also there is zero external wrench $\{\mathbf{W}_{EXT}\}$.

Examples discussion: Snapshot example 1 requires three zero-tension (slack) cables and Snapshot example 2 requires an impossible negative tension on cable 4 (and a very low positive tension on cable 2). In the Trajectory example, cables tensions 2, 4, and 6 require impossible negative tensions for roughly half of the motion range (in different phases). The initial conclusion is that the nominal straight-line cables model for the FAST cable-suspended robot is of NO USE, and that the models with cable sag are REQUIRED for success. The reason is that the straight-line cables model has no model redundancy since the robot is underconstrained (requiring gravity in attempt to maintain positive cable tensions), but the cable-sag model (Li et al., 2013) has kinematics/statics interactions, employs nine state variables, and thus allows room for optimization of positive cable tensions.

Figures 11a and 11b show two improved FAST cable-arrangement designs, in the sense that the straight-line model yields acceptable pseudostatics results (not included) with only positive cable tensions for simulated motions throughout the respective workspaces. Figure 11a is based on the RoboCrane cable arrangement design (Albus et al., 1993). Figure 11b is based on a crossed-cable design, for which cable interference may be an issue.

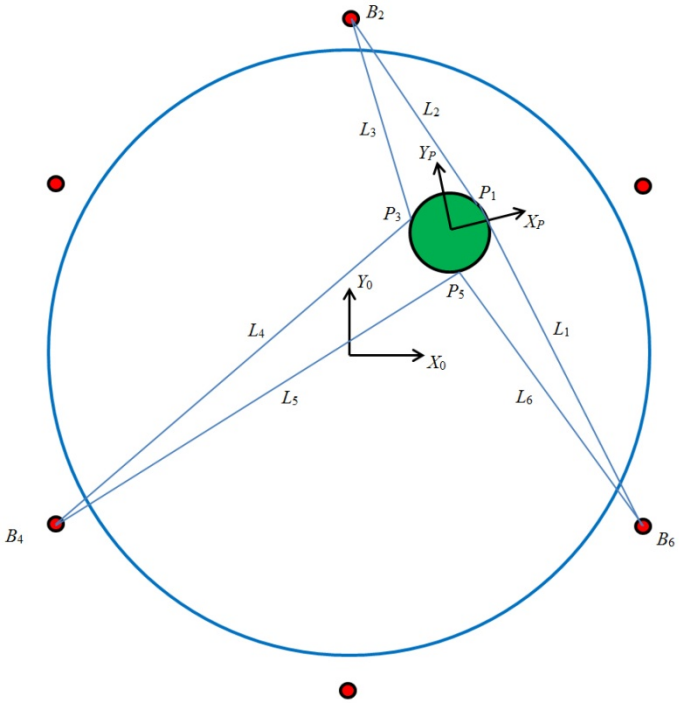

Figure 11a. Alternative FAST Design based on the NIST RoboCrane Cable Arrangement (Albus et al., 1993)

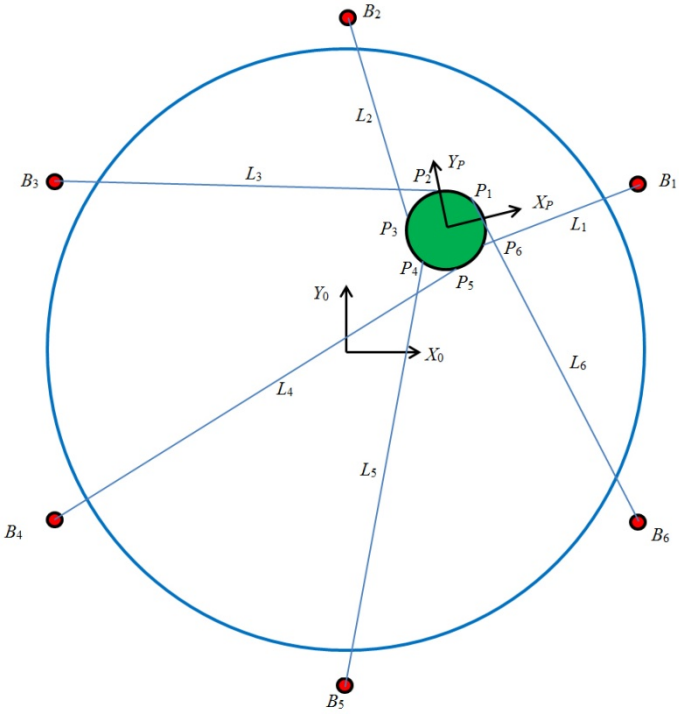

Figure 11b. Alternative FAST Design based on a Crossed-Cable Design

Presumably the 50 m one-tenth scale experimental hardware built by the FAST team and under testing at Miyun Station has led to confidence that the cable-sag model will allow robot operation with only positive cable tensions (i.e. validations have been done). Due to complex nonlinear dynamics, there is no guarantee that the results and designed controller will scale easily to the full-size FAST robot, but hopefully the cable tensions issues will be safe.

8. CONCLUSION

This paper has presented a comparison of two large radio telescopes: Arecibo vs. the designed FAST system. The Arecibo cable-suspension is static, while the FAST design includes a 6-dof underconstrained cable-suspended robot to position and orient its focus cabin. A straight-line cable model was presented for the FAST robot kinematics and statics, intended as a baseline for the more complicated model including cable sag. In presenting examples it was discovered that the straight-line model is of no use since it always yields some negative cable tensions over the required FAST workspace. Therefore, the cable-sag model MUST be used since it allows for optimization to try to avoid slack cables. Two alternative cable-arrangement designs were presented for FAST which overcome the problem of negative cable tensions when using the straight-line cable pseudostatics model.

ACKNOWLEDGEMENTS

This work was conducted during the author's sabbatical from Ohio University at the University of Puerto Rico, Mayaguez. The author gratefully acknowledges financial support from Ricky Valentin, UPR ME chair, and the Russ College of Engineering & Technology at Ohio University.

REFERENCES

J. Albus, R. Bostelman, and N. Dagalakis, 1993, "The NIST RoboCrane", Journal of National Institute of Standards and Technology, 10(5): 709-724.

P.M. Bosscher, R.L. Williams II, L.S. Bryson, and D. Castro-Lacouture, 2007, "Cable-Suspended Robotic Contour Crafting System", Journal of Automation in Construction, 17: 45-55.

P.D. Campbell, P.L. Swaim, and C.J. Thompson, 1995, "Charlotte Robot Technology for Space and Terrestrial Applications", 25th International Conference on Environmental Systems, San Diego.

L.L. Cone, 1985, "Skycam: An aerial robotic system", BYTE, October.

J.J. Craig, 2005, Introduction to Robotics: Mechanics and Control, Addison Wesley Publishing Co., Reading, MA.

K. Kozak, Q. Zhou, and J. Wang, 2006, “Static Analysis of Cable-Driven Manipulators with Non-Negligible Cable Mass”, IEEE Transactions on Robotics, 22(3): 425-433.

H. Li, X. Zhang, R. Yao, J. Sun, G. Pan, and W. Zhu, 2013, “Optimal Force Distribution Based on Slack Rope Model in the Incompletely Constrained Cable-Driven Parallel Mechanism of FAST Telescope”, in Cable-Driven Parallel Robots Mechanisms and Machine Science, 12: 87-102.

H. Li, R. Nan, H. Kärcher, W. Zhu, J. Sun, M. Lazanowski, S. Kern, B. Strah, F.F. Womba, and C. Jin, 2008, “Working space analysis and optimization of the main positioning system of FAST cabin suspension”, Proceedings of SPIE, Astronomical Instrumentation, Ground-Based and Airborne Telescopes II, Marseille, 70120T-5: 1–11.

G. Meunier, B. Boulet and M. Nahon, 2009, “Control of an Overactuated Cable-Driven Parallel Mechanism for a Radio Telescope Application”, IEEE Transactions on Control Systems Technology, 17(5): 1043-1054.

R. Nan, D. Li, C. Jin, Q. Wang, L. Zhu, W. Zhu, H. Zhang, Y. Yue, and L. Qian, 2011, “The Five-Hundred-Meter Aperture Spherical Radio Telescope (FAST) Project”, International Journal of Modern Physics D, 20: 989:1024.

R. Nan, “Five-hundred-meter aperture spherical radio telescope (FAST)”, 2006, Science in China: Series G Physics, Mechanics & Astronomy, 49(2): 129–148.

B. Strah, S. Kern, F. Fomi, M. Lazanowski, H. Li, R. Nan, H. Kärcher, and R. Nordmann, 2008, “Trajectory Control of Cable Suspended FAST Telescope Focus Cabin”, Proceedings of SPIE, Advanced Optical and Mechanical Technologies in Telescopes and Instrumentation, 7018: 1–12.

R.L. Williams II, 1992, "Kinematics of an In-Parallel Actuated Manipulator Based on the Stewart Platform Mechanism", NASA Technical Memorandum 107585, NASA Langley Research Center, Hampton, VA, March.

APPENDIX. Arecibo vs. FAST Radio Telescopes Graphical Comparisons

MATLAB

The top and front views of the Arecibo and FAST Radio Telescopes are shown below in MATLAB simulation for direct comparison. All MATLAB graphics are to scale and all viewing windows are identical. All pertinent dimensions were presented in the paper and the "ground level" is $Z = 0$ in both front views.

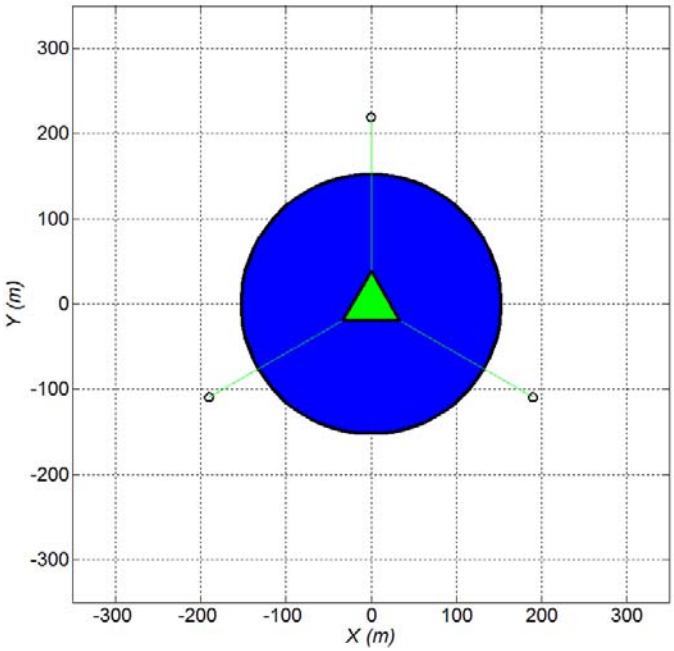

Figure A.1 Arecibo Top View

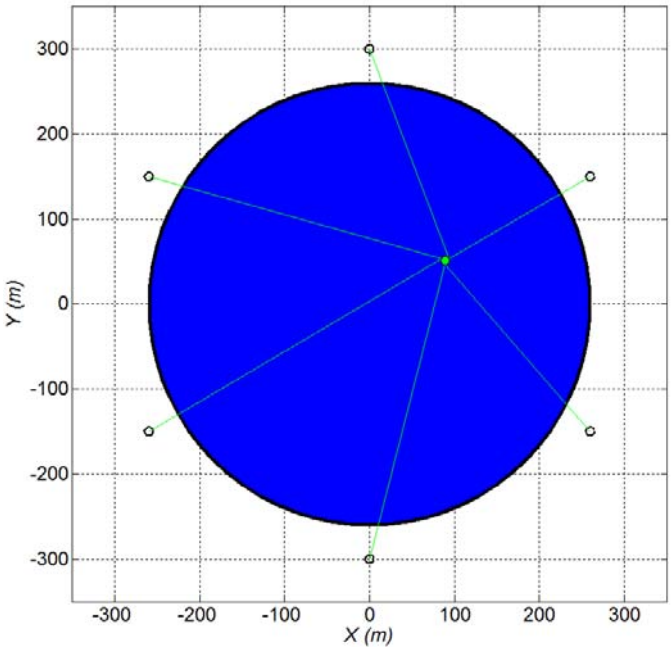

Figure A.2 FAST Top View

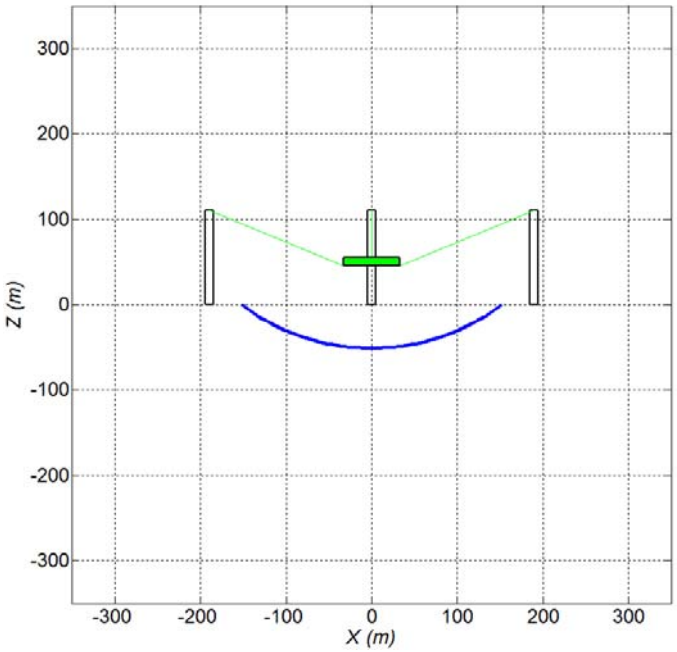

Figure A.3 Arecibo Front View

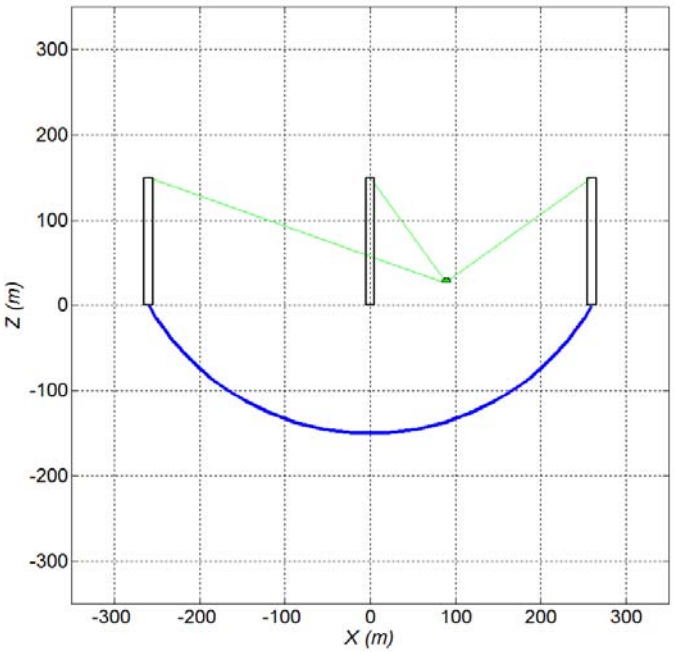

Figure A.4 FAST Front View

Ohio University Convocation Center Comparison

The satellite view of the campus of Ohio University in Athens, Ohio, USA, is shown below, with the footprints of the Arecibo and FAST Radio Telescopes at correct scale for direct comparison. The Convocation Center is a huge building, with 13,500 seats for college basketball and graduation, etc.

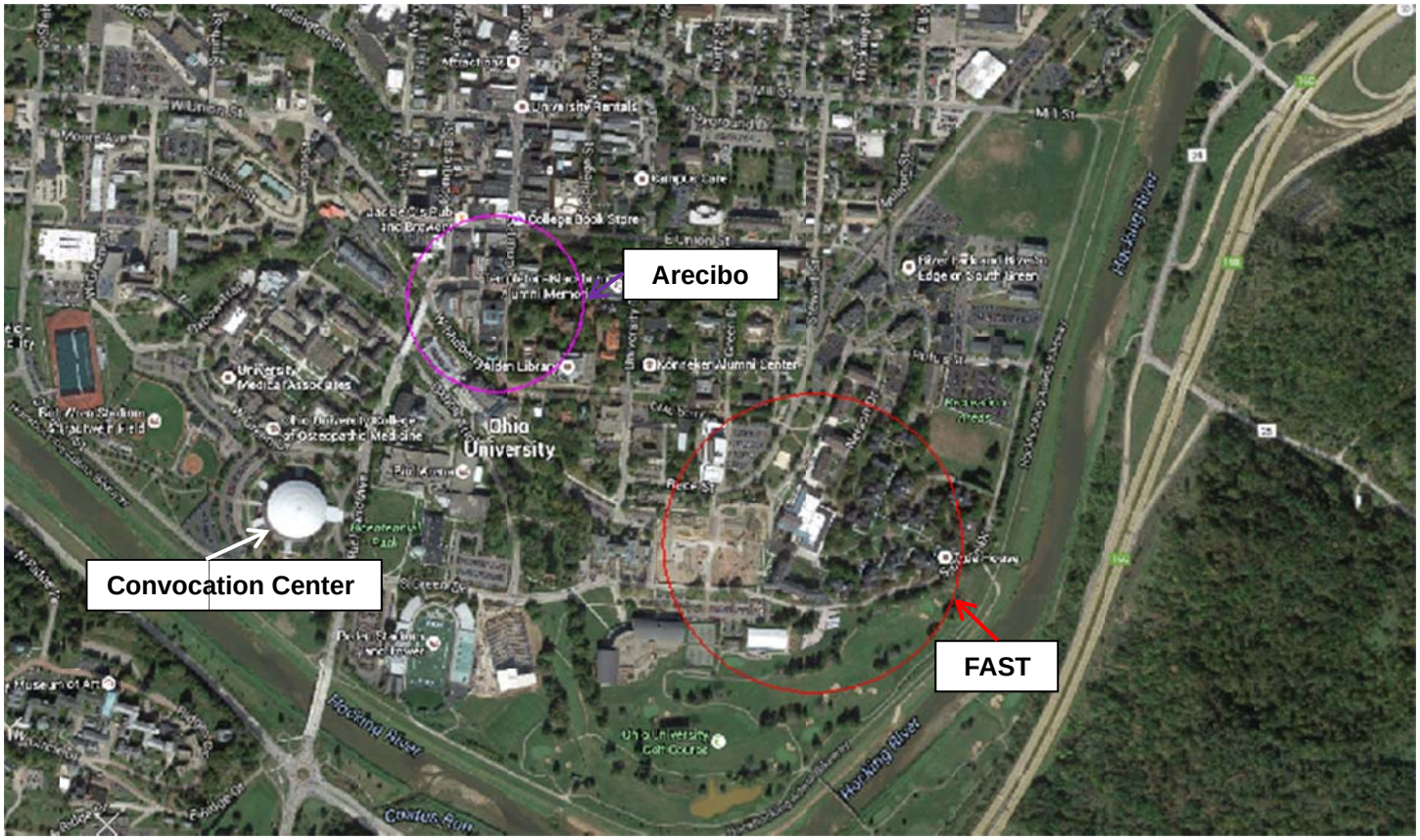

Structure	Diameter (m)	Footprint Area (acres)
Convocation Center	100	1.9
Arecibo Observatorio	305	18.1
FAST Space Telescope	520	52.5